frontiers | Frontiers in Soil Science

TYPE Original Research
PUBLISHED 10 July 2025
DOI 10.3389/fsoil.2025.1639967

OPEN ACCESS

EDITED BY
Xinqiang Liang,
Zhejiang University, China

REVIEWED BY
Zhuang Ge,
Dalian University, China
Sangar Khan,
Ningbo University, China

*CORRESPONDENCE
Xiaoyan Qian
17612247484@163.com

RECEIVED 03 June 2025
ACCEPTED 23 June 2025
PUBLISHED 10 July 2025

CITATION
Zhang S, Yang Y, Zhang J and Qian X (2025) Mitigating salt stress in saline-alkali soils through co-application of superabsorbent carbon-based material and flue gas desulfurization gypsum.
Front. Soil Sci. 5:1639967.
doi: 10.3389/fsoil.2025.1639967

Mitigating salt stress in saline-alkali soils through co-application of superabsorbent carbon-based material and flue gas desulfurization gypsum

Shengnan Zhang[1,2], Youming Yang[1], Juanxiang Zhang[1,2] and Xiaoyan Qian[1,2]*

[1]College of Water Resources and Architecture Engineering, Tarim University, Xinjiang, China, [2]Key Laboratory of Tarim Oasis Agriculture (Tarim University), Ministry of Education, Alaer, China

Flue gas desulfurization gypsum (FGD) and biochar are considered effective amendments for alleviating soil salinity stress. However, the co-application of these amendments in practice requires further investigation. This study successfully prepared a superabsorbent carbon-based material (CB) via graft polymerization and applied it in combination with FGD to investigate their effects on leaching salt ions and improving saline-alkali soil. A laboratory soil column leaching experiment was conducted with six treatments: control (CK, no amendment), cotton straw biochar (BC), CB, FGD, BC+FGD, and CB+FGD. Field plot trials were further employed to evaluate the soil amendment efficacy. The results demonstrated that the co-application of the CB and FGD significantly alleviated salt stress by promoting Na^+ leaching. During the P1 (sharp decrease) leaching phase, Na^+ leaching concentrations under the sole FGD and CB+FGD treatments increased by 89.08% and 90.92%, respectively, compared to CK. Co-application with FGD significantly increased the content of Ca^{2+} and SO_4^{2-} in the soil. The CB effectively retained soil K^+, and the Cl^- content after leaching was significantly lower than in CK. Field trials further confirmed that the co-application of the CB and FGD significantly reduced the contents of Na^+, Cl^-, and Mg^{2+} while increasing the contents of Ca^{2+}, K^+, and SO_4^{2-}. The contents of Na^+, Cl^-, and K^+ increased with soil depth, indicating the migration of major salt ions towards deeper soil layers with water movement. The CB+FGD treatment significantly reduced soil TSS, electrical conductivity (EC), and SAR. In conclusion, the co-application between the CB and FGD enhances salt leaching efficiency and soil water retention capacity, exerting a positive influence on the remediation of saline-alkali soils. This study provides a novel strategy for utilizing agricultural waste in saline soil management.

KEYWORDS

saline-alkali soil, superabsorbent carbon-based material, flue gas desulfurization gypsum (FGD), salt suppression, leaching efficiency

1 Introduction

Soil salinization has become a major factor in global soil degradation (1). Globally, salinized land covers approximately 1.7×10^9 hectares (2), with nearly 100 million hectares located in China, primarily distributed across arid and semi-arid regions (3). Soil salinization leads to poor soil nutrient availability and low utilization efficiency, thereby adversely affecting crop yields and posing a significant constraint to global agricultural production (4). Nevertheless, saline-alkali soils possess substantial potential for development and utilization, making their amelioration crucial for achieving sustainable agriculture. Traditional reclamation techniques, such as leaching and salt drainage, cultivating salt-tolerant crops, and applying soil amendments, suffer from limitations including high water dependency, susceptibility to amendment loss, and concurrent depletion of soil nutrients (3).

Biochar is a carbon-rich material produced through the pyrolysis of organic waste (3). It is recognized as an effective amendment for alleviating salt stress in soils and has been widely applied to improve soil properties (1, 5–7). Studies indicate that biochar can enhance soil nutrients, promote crop growth, and increase crop yield (8–10). However, the influence of biochar on soil water retention and salt suppression characteristics primarily depends on the feedstock (10), pyrolysis conditions (11), particle size (12, 13), application rate (10, 14), and soil type (13). Furthermore, its effectiveness is constrained by its internal pore structure, specific surface area, and the content of hydrophobic functional groups (10–14), resulting in inherently limited water retention and salt suppression potential. Its application in saline soils may even exacerbate the loss of soil moisture and nutrients. Therefore, our research team previously synthesized three types of superabsorbent carbon-based materials using biochar combined with chitosan and sodium alginate. These materials demonstrated excellent water absorption properties (15).

Superabsorbent carbon-based materials are a novel class of biochar-based soil amendments prepared through physical or chemical methods. Characterized by high water absorption capacity and unique pore structures, they are cross-linked hydrophilic polymers exhibiting superior water absorption and retention potential (14). Their key features include high water absorption and retention capacity (16), large specific surface area (3), abundant functional groups (e.g., hydroxyl, carboxyl) (17), as well as good biocompatibility and environmental friendliness. In soil remediation, these materials can absorb and retain water, thereby improving soil moisture status and aggregate structure, enhancing soil aeration and nutrient retention capacity, creating a favorable micro-environment for crop growth (18, 19), and promoting root development (7, 17).

Due to their rich functional groups and porous structure, superabsorbent carbon-based materials can adsorb soil salt ions (e.g., Na^+, Cl^-) or reduce soil salinity by enhancing pore water flow, mitigating salt stress on plants (14, 20). Gypsum, composed of fine particles with low water content, can reduce salinity and alkalinity in saline-alkali soils and improve soil structure and permeability (1). Additionally, gypsum supplies essential mineral nutrients like Ca, S, and Si, aiding plant growth and enhancing seedling emergence rates and yields in saline lands (21). Co-application of flue gas desulfurization gypsum (FGD) in saline-alkali soils can regulate soil pH, replenish mineral elements, decrease salinity, and improve fertility, thereby helping to mitigate soil salinization/alkalization and promoting crop growth (22, 23).

However, research on the mechanisms by which carbon-based materials and FGD suppress salinity and retain water in saline-alkali soils is scarce. The efficacy varies considerably among different types of carbon-based materials (1, 10, 24), and the key factors governing their interaction with saline soils—such as application rate, particle size, and types of functional groups—remain unclear.

Given that superabsorbent carbon-based materials and FGD individually reduce salinity (1, 25), alleviate salt stress (26, 27), and enhance soil water retention (17, 19), we hypothesize that their co-application will synergistically improve salt leaching efficiency and soil water retention capacity in saline soils, surpassing the effects of individual applications. The primary objectives of this study are as follows: (1) To investigate the dynamic effects of applying the superabsorbent carbon-based material alone and in combination with FGD on salinity in saline soil; (2) To determine the optimal treatment involving the co-application of the superabsorbent carbon-based material and FGD; (3) To establish the causal relationships between soil salt ions and key soil physicochemical properties following the application of the superabsorbent carbon-based material alone and in combination with FGD.

2 Materials and methods

2.1 Study area description

The experimental site is located at Tarim University (40° 32'32"N, 81°17'11"E), Xinjiang Uygur Autonomous Region, situated in the hinterland of the Tarim Basin. The region experiences a typical warm-temperate continental climate characterized by extreme aridity, abundant sunshine, significant diurnal temperature variations, low precipitation, and high evaporation. The basin receives <100 mm average annual precipitation, while potential evaporation ranges from 1800–2900 mm (28). Mean annual temperature varies between 10.6–11.5°C, with recorded extremes of 43.6°C and -30.9°C (29). The predominant soils in the area are saline-alkali soils with an exchangeable sodium percentage (ESP) of 34.42%. Cotton is the main cultivated crop in this area.

2.2 Materials

The test soil was collected from saline-alkali soil within the experimental area. Soil samples were taken from the 0–20 cm depth profile, air-dried under natural conditions, sieved to remove impurities, and passed through a 2-mm sieve. The soil texture was classified as sandy loam (sand: 75.58%, silt: 24.03%, clay:

0.39%). The superabsorbent carbon-based material used in the experiments was synthesized through the following process: cotton straw was pyrolyzed under oxygen-limited conditions at 600°C to produce biochar (BC), which was subsequently crushed, sieved, and modified with chitosan to yield the chitosan-modified superabsorbent carbon-based material (CB) (15), facilitating the resource reuse of waste cotton stalks. Key material characterization data are provided in Supplementary Figures S1-S3. FGD was obtained from Alar Shengyuan Thermal Power Co., Ltd. The FGD material presented as an off-white powder (particle size: 30–60 μm) with calcium sulfate dihydrate ($CaSO_4{\cdot}2H_2O$) comprising >90% of its mass. The basic physicochemical properties of the test soil are presented in Table 1.

2.3 Experimental design

2.3.1 Salt leaching experiment

A one-dimensional vertical infiltration method with constant water head was employed to investigate the effects of carbon-based materials and their co-application with flue FGD on soil salt leaching. The experiment utilized plexiglass soil columns (inner diameter: 10 cm, height: 35 cm) connected to a Mariotte bottle water supply system (Figure 1). Six treatments were established: CK (control, no amendment), BC (cotton straw biochar alone), CB (chitosan-modified superabsorbent carbon-based material alone), FGD (flue gas desulfurization gypsum alone), BC+FGD, and CB +FGD. Amendments were uniformly mixed into the 0–20 cm soil layer at an application rate of 0.5% (w/w). Each soil column was filled to a height of 30 cm. For co-application treatments (BC+FGD and CB+FGD), FGD was added simultaneously. Each treatment was replicated three times. The initial breakthrough time of leachate was recorded following the methodology described by Yue et al. (30). Changes in the electrical conductivity (EC) of the leachate were dynamically monitored. Based on the characteristics of the EC decline, the leaching process was divided into three distinct phases: a rapid decline phase (P1, EC ≈ 60% of initial value), a gradual decline phase (P2, EC ≈ 90% of initial value), and a stable phase (P3). The experiment was terminated when the EC of the leachate decreased to 5 $mS{\cdot}cm^{-1}$ (corresponding to a total salt content of approximately 3 $g{\cdot}L^{-1}$) and stabilized.

2.3.2 Field experiment

Field experiments were conducted from April to November 2023 at the Water-saving Irrigation Experimental Station of Tarim University. PVC cylinders (top diameter: 29 cm, bottom diameter: 26 cm, height: 36 cm) were used. Nine evenly spaced aeration holes (diameter = 5 mm) were drilled in the bottom. Each cylinder was filled with soil to a depth of 30 cm. Amendments (superabsorbent CB and/or FGD) were incorporated into the top 0–20 cm soil layer. Six treatments were established (identical to those described in Section 2.3.1 for the column leaching experiment). Cotton (*Gossypium hirsutum L.* cv. 'Tahe No. 2') was planted, with two seedlings per cylinder. During the entire cotton growth period, irrigation was applied 12 times (total irrigation amount: 3000 $m^3{\cdot}ha^{-2}$; single application: 250 $m^3{\cdot}ha^{-2}$; interval: 6–7 days). Compound fertilizer (15-15–15 $N\text{-}P_2O_5\text{-}K_2O$) was applied as basal dressing at 5.4 g per column. Conventional topdressing (urea + compound fertilizer) was subsequently applied with irrigation at rates of 375 kg N ha^{-1}, 450 kg P_2O_5 ha^{-1}, and 150 kg K_2O ha^{-1}. Fertilization and all other cultivation and management practices were consistent across all treatments and aligned with local field practices. Each treatment was replicated three times.

2.4 Measurements and methods

Salt ion concentrations (K^+, Na^+, Ca^{2+}, Mg^{2+}, HCO_3^-, SO_4^{2-}, and Cl^-) were determined in the leachate collected during each leaching phase and in the soil layers after leaching. For the field experiment, soil salt ion concentrations at depths of 0–20 cm and 20–30 cm within the cylinders were measured at seeding stage, bud stage, flowering and boll stage, boll-opening stage. Soil EC was measured at the boll-opening stage. K^+ and Na^+ were determined by flame photometry (AP-1200, Shanghai Precision Instrument Co., China). Ca^{2+} and Mg^{2+} were determined by EDTA complexometric titration (10). HCO_3^- was determined by acid-base titration (31). SO_4^{2-} was determined by indirect EDTA titration (32). Cl^- was determined by silver nitrate titration (31). Total soluble salts (TSS) were calculated as the sum of the concentrations of water-soluble anions and cations. The sodium adsorption ratio (SAR) was calculated using Equation 1 (33):

$$SAR = \frac{[Na^+]}{\sqrt{\frac{[Ca^{2+}]+[Mg^{2+}]}{2}}} \quad (1)$$

Where $[Na^+]$, $[Ca^{2+}]$ and $[Mg^{2+}]$ are the concentrations ($mmol{\cdot}L^{-1}$) of sodium, calcium, and magnesium ions in the soil solution.

2.5 Data processing and analysis

Experimental data are expressed as the mean ± standard deviation (SD) of three replicates. Statistical analyses were

TABLE 1 Basic physicochemical properties of the test soil.

Soil layers (cm)	pH	Bulk density ($g{\cdot}cm^{-3}$)	Saturated moisture (%)	Electrical conductivity ($mS{\cdot}cm^{-1}$)	Na^+	K^+	Ca^{2+}	Mg^{2+}	Cl	SO_4^{2-}	HCO_3
					($g{\cdot}kg^{-1}$)						
0–20	7.40	1.40	43	1.12	2.43	0.87	2.69	1.07	0.33	1.89	0.79

pH, EC, and ions of the soil were measured on saturated extract.

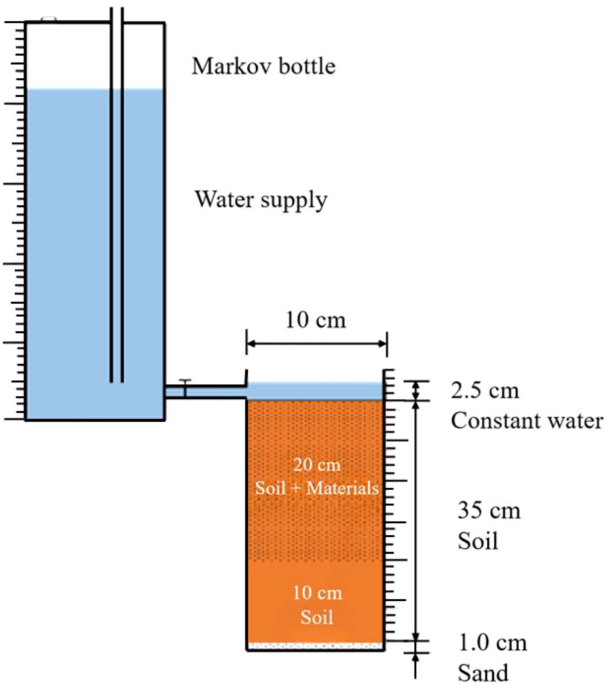

FIGURE 1
Schematic diagram of the salt leaching test.

performed using SPSS 26.0 software. One-way analysis of variance (ANOVA) was employed to assess significant differences among treatments at the $p < 0.05$ significance level. Origin 2021 software was used for graphing and correlation analysis.

3 Results

3.1 Effects of different carbon-based materials on salt leaching in the column experiment

3.1.1 Dynamics of cation leaching

Figure 2 illustrates the effects of applying carbon-based materials alone or in combination with flue FGD on the leaching concentrations of major cations (Na^+, K^+, Mg^{2+}, and Ca^{2+}) in the leachate. Significant differences in the concentrations of Na^+, K^+, Ca^{2+}, and Mg^{2+} were observed among all treatments (Figures 2a–d). Compared to the control (CK), both carbon-based materials and FGD significantly enhanced Na^+ leaching, with the co-application treatments showing superior effects to single applications. The CB +FGD co-application demonstrated the greatest efficacy, driving peak increases in leachate Na^+ concentration of 114.19% and 97.33% compared to CK and BC, respectively. Na^+ leaching predominantly occurred during the P1 (rapid decline) phase. Here, FGD alone and CB+FGD exhibited the most pronounced enhancement, increasing Na^+ leaching by 89.08% and 90.92%, respectively, relative to CK. During the P2 (gradual decline) phase, leaching amounts for all treatments were significantly higher than CK, with CB+FGD showing the largest increase (101.37%). In the P3 (stable) phase, treatment differences were distinct, and CB+FGD increased Na^+ leaching concentration by 226.23%.

Application of CB alone and CB+FGD promoted K^+ leaching compared to CK, increasing concentrations by 25.24% and 12.19%, respectively. Conversely, other treatments suppressed K^+ leaching, indicating that FGD co-application reduced K^+ concentration in the leachate. K^+ leaching followed the order P1 > P2 > P3 across all phases. Both carbon-based materials and FGD enhanced Ca^{2+} leaching (co-application > single application), with CB+FGD showing the greatest increase (44.65%). Similarly, carbon-based materials and FGD significantly improved Mg^{2+} leaching compared to CK (single application > co-application). BC and BC+FGD treatments were most effective for Mg^{2+} leaching, achieving increases of 121.16% and 111.11% versus CK, respectively. Compared to sole FGD, these treatments showed significantly higher Mg^{2+} leaching rates (+32.70% and +26.67%, respectively). Leaching of Mg^{2+} induced by carbon-based materials primarily occurred during the P2 and P3 phases. Co-application with FGD reduced the Mg^{2+} leaching effect of CB in the CB+FGD treatment.

In summary, both carbon-based materials and FGD promoted the leaching of Na^+, Ca^{2+}, and Mg^{2+}. However, FGD co-application specifically enhanced Na^+ leaching while simultaneously suppressing the leaching of Ca^{2+}, Mg^{2+}, and K^+. A decreasing trend in cation concentrations from the P1 to P3 phase suggests that the amendments alleviated salt stress in the saline soil.

3.1.2 Dynamics of anion leaching

Figure 3 shows the effects of different carbon-based materials and FGD co-application on the leaching concentrations of major anions (HCO_3^-, Cl^-, and SO_4^{2-}) in the leachate. Compared to CK, BC, FGD, and BC+FGD had no significant effect on HCO_3^- leaching. Sole CB application was most effective for HCO_3^- leaching, increasing leachate concentration by 144.81% and 98.85% compared to CK and BC. Conversely, FGD co-application reduced HCO_3^- concentration in the leachate, with CB+FGD showing the largest decrease (74.06%). HCO_3^- leaching was primarily concentrated in the P1 phase.

All treatments significantly promoted the leaching of Cl^- and SO_4^{2-} compared to CK across all leaching phases (co-application > single application). CB+FGD was the most effective treatment, increasing Cl^- and SO_4^{2-} concentrations by 105.29% and 155.42%, respectively. Compared with CB, the increases of Cl^- and SO_4^{2-} reached 14.78% and 11.73%. These results indicate that the treatments facilitated anion leaching to varying degrees, thereby reducing the accumulation of harmful ions in the saline soil.

3.1.3 Post-leaching cation distribution in soil profile

Figure 4 depicts the effects of carbon-based materials and FGD co-application on the distribution of major cations (Na^+, K^+, Mg^{2+}, Ca^{2+}) within the soil profile after leaching. Application of carbon-based materials and FGD significantly reduced Na^+ content in all soil layers (co-application > single application), with CB+FGD showing the maximum reduction (40.43%). Na^+ content generally increased with soil depth, except in the BC treatment. Compared to

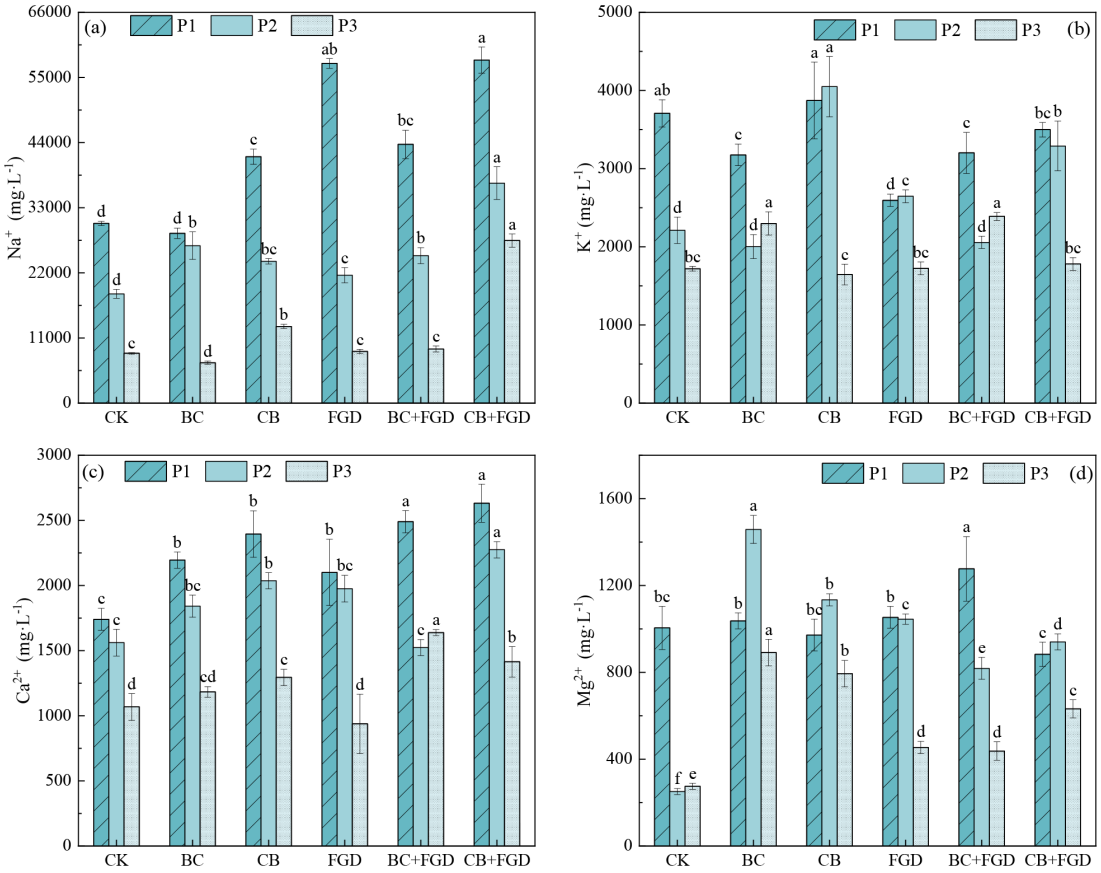

FIGURE 2
The effects of carbon-based materials and their combined application of FGD on the main cations, such as Na^+ **(a)**, K^+ **(b)**, Ca^{2+} **(c)**, and Mg^{2+} **(d)** in the eluent during the rinsing stages P1, P2 and P3. The error bar represents ± standard deviation, and different lowercase letters indicate significant differences in different treatments at the same rinsing stage ($p < 0.05$).

CK, single application of carbon-based materials and FGD co-application significantly reduced K^+ content in the 0–20 cm layer, with CB alone causing the largest decrease (38.81%). Single FGD application increased K^+ content. BC and BC+FGD treatments resulted in significantly higher K^+ content in the 20–30 cm layer compared to other treatments.

Carbon-based materials and FGD significantly enhanced the retention of Ca^{2+} in the soil. Increases were particularly notable for FGD, BC+FGD, and CB+FGD treatments, and Ca^{2+} content generally increased with soil depth. Treatments other than CB and FGD alone reduced soil Mg^{2+} content compared to CK. FGD co-application had no significant impact on Mg^{2+} leaching.

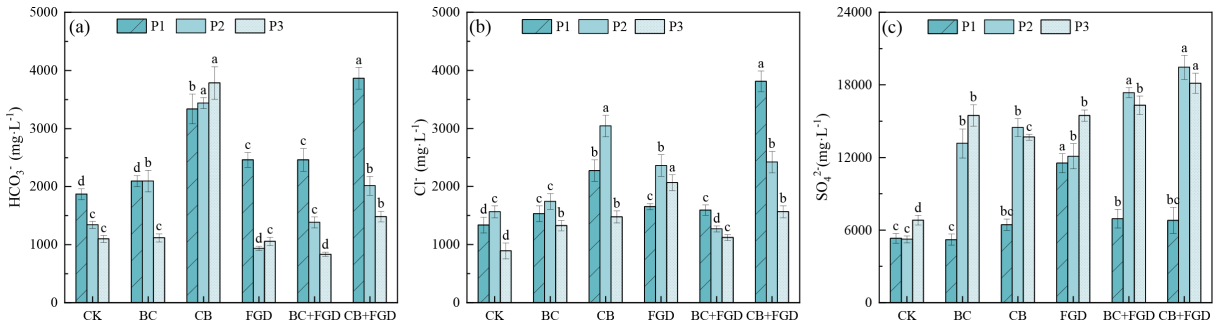

FIGURE 3
The effects of different carbon-based materials and their combined application of FGD on the main anions, such as HCO_3^- **(a)**, Cl^- **(b)**, and SO_4^{2-} **(c)** in the eluent during the rinsing stages P1, P2 and P3. The error bar represents ± standard deviation, and different lowercase letters indicate significant differences in different treatments at the same rinsing stage ($p < 0.05$).

10.3389/fsoil.2025.1639967

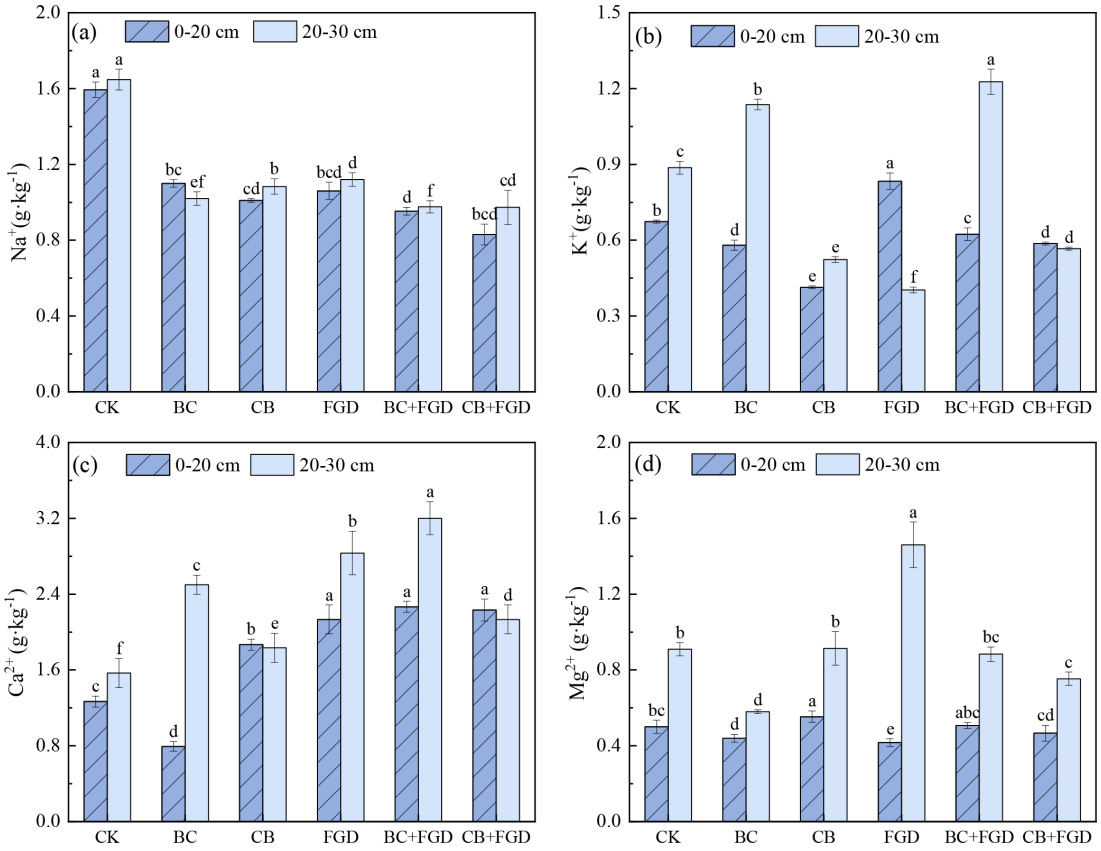

FIGURE 4
The effects of different carbon-based materials and their combined application of FGD on the main cations, such as Na^+ **(a)**, K^+ **(b)**, Ca^{2+} **(c)**, and Mg^{2+} **(d)** in different soil layer profiles. The error bar represents ± standard deviation, and different lowercase letters indicate significant differences in different treatments at the same rinsing stage ($p < 0.05$).

The highest Mg^{2+} content in the 0–20 cm and 20–30 cm layers was observed in the CB and FGD treatments, respectively.

3.1.4 Post-leaching anion distribution in soil profile

Figure 5 shows the effects of carbon-based materials and FGD co-application on the distribution of major anions (HCO_3^-, Cl^-, SO_4^{2-}) within the soil profile after leaching. FGD co-application significantly reduced soil HCO_3^- concentration. In the 0–20 cm layer, BC+FGD and CB+FGD treatments showed significant decreases (41.67% and 40.28%, respectively). In the 20–30 cm layer, CB+FGD caused the most significant reduction (13.16%). Carbon-based materials and FGD significantly decreased soil Cl^- concentration compared to CK (co-application > single application), with CB+FGD being the most effective. Cl^- content was markedly reduced in the 0–20 cm layer across treatments, while BC and FGD significantly increased Cl^- in the 20–30 cm layer.

Both carbon-based materials and FGD reduced soil SO_4^{2-} concentration (single application > co-application), with CB showing the largest decrease (30.33%). Single application of carbon-based materials had no significant effect on SO_4^{2-} in the 0–20 cm layer, but significantly lowered its content compared to CK in the 20–30 cm layer.

3.2 Dynamics of salt ions in field soil

3.2.1 Dynamics of cations in field soil

Figure 6 illustrates the changes in major cations (Na^+, K^+, Mg^{2+}, Ca^{2+}) across different soil layers in saline soil treated with carbon-based materials and FGD co-application during various cotton growth stages. Compared to CK, the addition of carbon-based materials and FGD reduced Na^+ and Mg^{2+} contents to varying degrees, while Ca^{2+} exhibited an opposite trend. K^+ content in BC, CB, and CB+FGD treatments showed an increasing trend at different stages. With the exception of Na^+, co-application with FGD generally led to increasing cation concentrations with soil depth. Na^+ content in the 0–20 cm layer decreased significantly as the cotton growth progressed. FGD co-application significantly reduced Na^+ content in all layers, with CB+FGD showing the largest reduction (37.90%). K^+ content in all layers initially increased and then decreased during the cotton growth period. Adding CB (except at the seedling stage) resulted in higher K^+ content than CK throughout the growth stages. FGD and BC+FGD treatments consistently had significantly lower K^+ content than CK across all growth stages. Carbon-based materials and FGD significantly increased Ca^{2+} content in all soil layers during all growth stages (co-application > single application), with CB+FGD

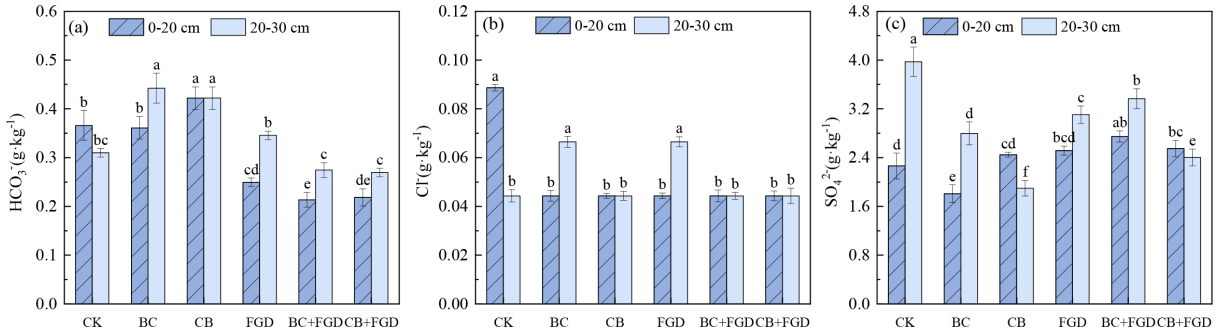

FIGURE 5
The effects of different carbon-based materials and their combined application of FGD on the main anions, such as HCO_3^- **(a)**, Cl^- **(b)**, and SO_4^{2-} **(c)** in different soil layer profiles. The error bar represents ± standard deviation, and different lowercase letters indicate significant differences among different treatments in the same soil layer (p< 0.05).

showing the maximum increase. Carbon-based materials maintained Mg^{2+} content below CK levels throughout the growth period, reaching its minimum at the boll-opening stage. Both FGD and CB+FGD reduced Mg^{2+} content by 11.77% compared to CK.

3.2.2 Dynamics of anions in field soil

Figure 7 shows the changes in major anions (HCO_3^-, Cl^-, SO_4^{2-}) across different soil layers in saline soil treated with carbon-based materials and FGD co-application during various cotton growth stages. Compared to CK, the amendments decreased HCO_3^- and Cl^- contents to varying degrees, while SO_4^{2-} showed an opposite trend. Except for SO_4^{2-}, co-application with FGD generally resulted in increasing anion concentrations with soil depth. HCO_3^- content decreased significantly as the cotton growth progressed, reaching its lowest level at the boll-opening stage. FGD co-application significantly reduced HCO_3^- content in the 0–20 cm layer, with CB+FGD showing the largest decrease. Cl^- content in all layers showed an increasing trend during the growth period and increased significantly with soil depth. FGD co-application significantly reduced Cl^- content in all layers of the saline soil, with CB+FGD again showing the largest reduction. Carbon-based materials and FGD significantly increased SO_4^{2-} content in the saline soil (co-application > single application), with CB+FGD exhibiting the greatest increase. SO_4^{2-} content decreased significantly as the cotton growth progressed but showed no clear trend with increasing soil depth.

3.2.3 Dynamics of soil physicochemical properties

Application of carbon-based materials and FGD significantly improved soil properties in the 0–20 cm layer (Figure 8). These treatments significantly reduced TSS at the seedling stage, although the effect was less pronounced or non-significant in the subsequent three growth stages (Figure 8a). Single amendments generally led to larger TSS reductions than co-application treatments, with CB showing the highest decrease (14.15%), possibly due to the introduction of ions like Mg^{2+} and Ca^{2+} from FGD. TSS gradually decreased throughout the cotton growth period across all treatments. Soil EC, which was positively correlated with TSS, exhibited a similar decreasing trend over the growth period (Figure 8b). Compared to CK, carbon-based materials and FGD significantly reduced soil EC. However, EC values in FGD co-application treatments were consistently higher than those with single carbon-based material applications, and single FGD application resulted in the smallest EC reduction. The SAR, reflecting the soil's capacity to counteract Na^+ alkalinity with Ca^{2+} and Mg^{2+}, was significantly lower in amended soils compared to CK (Figure 8c). Co-application effects were markedly superior to single applications. CB+FGD showed the largest SAR reduction, decreasing it by 34.74%, 31.61%, 38.15%, and 41.02% at the seedling, Bud, flowering and boll, and boll-opening stages, respectively.

Figure 8 also reflects the correlations between soil physicochemical indicators and salt ions. A highly significant positive correlation (R^2 = 0.52, p < 0.01) was observed between EC and TSS, confirming EC as an indirect measure of soil salinity. Na^+, Ca^{2+}, Cl^-, and SO_4^{2-} showed highly significant positive correlations (p < 0.001) with TSS, identifying them as major contributors to salinity. SAR exhibited a strong positive correlation with Na^+ (R^2 = 0.98, p < 0.001) and significant negative correlations with Ca^{2+} (R^2=-0.69, p < 0.01) and Mg^{2+} (R^2=-0.58, p < 0.01). These results demonstrate the antagonistic role of Ca^{2+} and Mg^{2+} in countering Na^+ toxicity. Reducing exchangeable Na^+ while applying calcium-based amendments represents an effective saline-alkali soil reclamation strategy. HCO_3^- showed a weak negative correlation with SAR (p < 0.05), potentially due to reduced dissolved salt content from carbonate precipitation under alkaline conditions. K^+ showed no significant correlation with salinity indicators, reflecting its tendency for adsorption or plant uptake and its low contribution to salt stress.

4 Discussion

4.1 Dynamics of salt ions in leachate

This study primarily investigated the effects of carbon-based materials and FGD on salt dynamics within the 0–30 cm profile of saline soil. The dominant ions contributing to salinity in the study

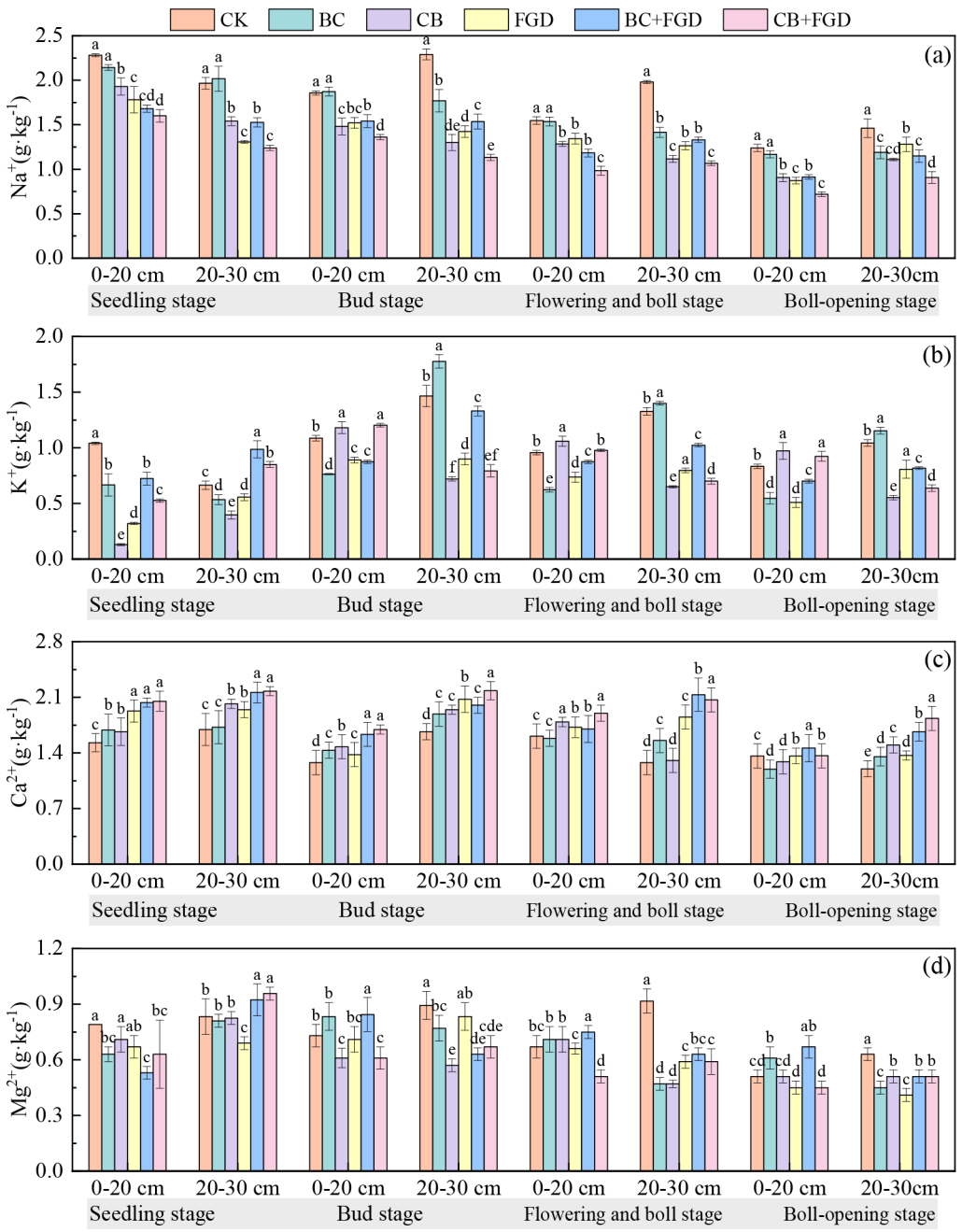

FIGURE 6
Effects of different carbon-based materials and their combined application of FGD on cations, such as Na^+ **(a)**, K^+ **(b)**, Ca^{2+} **(c)**, and Mg^{2+} **(d)** in different soil layers. The error bar represents ± standard deviation, and different lowercase letters indicate significant differences in different treatments at the same rinsing stage ($p < 0.05$).

area were Na^+, Ca^{2+}, Mg^{2+}, SO_4^{2-}, and Cl^- (Table 1, Figure 8d). The application of carbon-based materials and FGD significantly enhanced the leaching of these salt ions (Figures 2, 3), consistent with findings from previous studies (25, 34). Co-application of carbon-based materials with flue FGD generally outperformed single applications in promoting ion leaching, resulting in higher cumulative amounts of dissolved Na^+, Ca^{2+}, SO_4^{2-}, and Cl^- in the leachate. The chitosan-modified superabsorbent carbon-based material co-applied with FGD (CB+FGD) exhibited the most pronounced effect, significantly enhancing the leaching of Na^+, Ca^{2+}, SO_4^{2-}, and Cl^- compared to other treatments. The overall leaching efficacy followed the order: co-application > single application > control (CK).

The porous structure and high specific surface area (SSA) of carbon-based materials facilitate the adsorption of salt ions within their pores, thereby reducing total soil salinity and promoting ion elution (35). Furthermore, they enhance soil aggregate formation and increase total porosity (18, 22, 36), improving the physical

10.3389/fsoil.2025.1639967

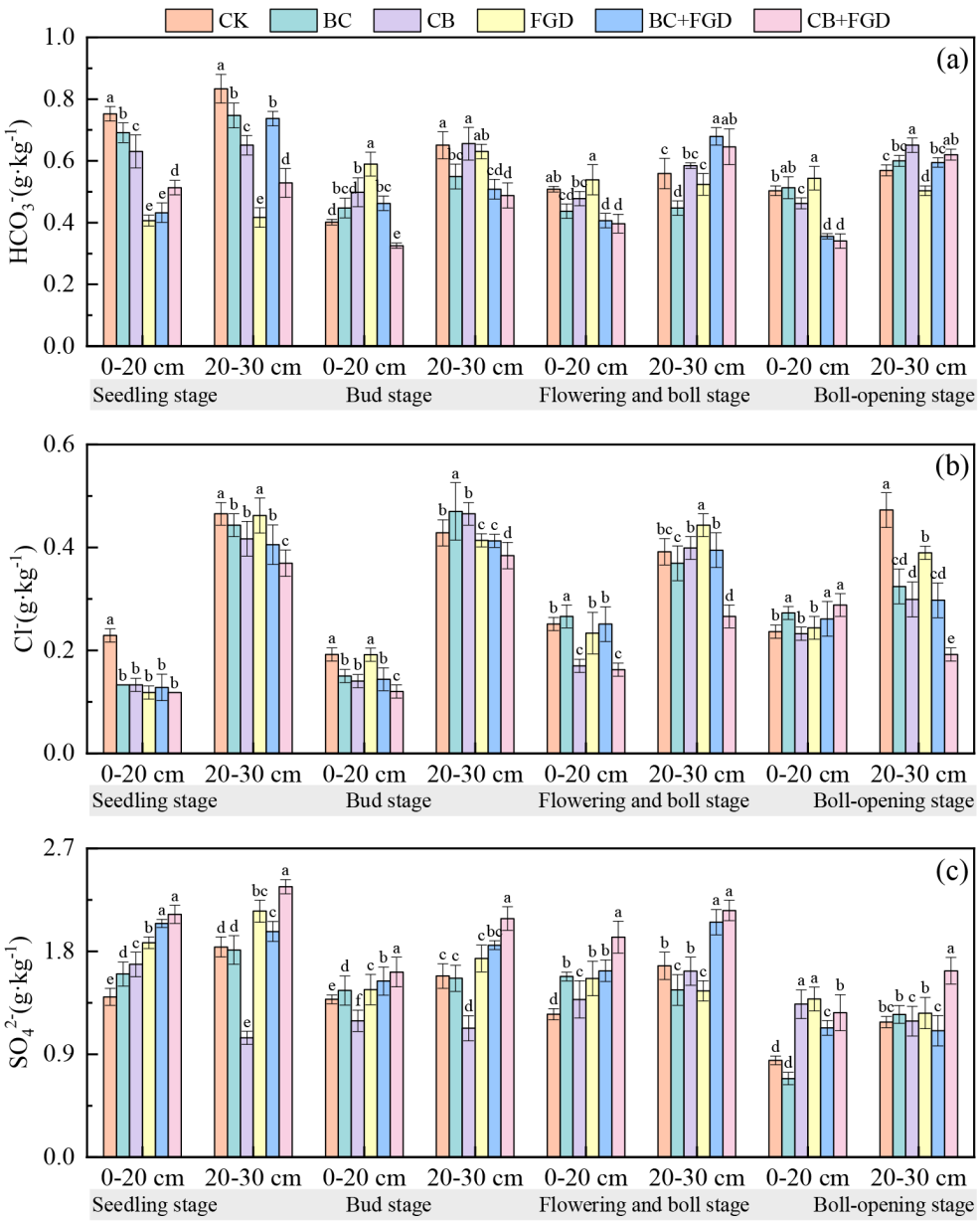

FIGURE 7
Effects of different carbon-based materials and their combined application of FGD on anions, such as HCO_3^- **(a)**, Cl^- **(b)**, and SO_4^{2-} **(c)** in different soil layers. The error bar represents ± standard deviation, and different lowercase letters indicate significant differences in different treatments at the same rinsing stage ($p < 0.05$).

structure of saline-alkali soil. This modification increases the viscosity coefficient of the soil solution, retards water movement, and ultimately enhances salt leaching efficiency (30). The superabsorbent carbon-based material (CB), possessing a larger SSA and superior water absorption and retention capabilities (15), demonstrated more significant leaching effects (18, 19). Concurrently, Ca^{2+} and Mg^{2+} introduced by the carbon-based materials can displace exchangeable Na^+ from soil colloids via cation exchange, further improving leaching efficiency (37).

Co-application with FGD augmented the leaching of Na^+, Ca^{2+}, and SO_4^{2-} by the carbon-based materials. This co-application effect likely stems from the primary component of FGD, $CaSO_4{\cdot}2H_2O$, which significantly increases soil Ca^{2+} and SO_4^{2-} concentrations. Consequently, the leaching amounts of Ca^{2+} and SO_4^{2-} in the leachate rise substantially. The additional Ca^{2+} also displaces exchangeable Na^+ adsorbed onto soil colloids, further promoting Na^+ leaching (38).

4.2 Distribution of salt ions in soil profile post-leaching

Removing major salt ions like Na^+ and Cl^- is crucial for ameliorating soil salinity. Both single and co-applications of

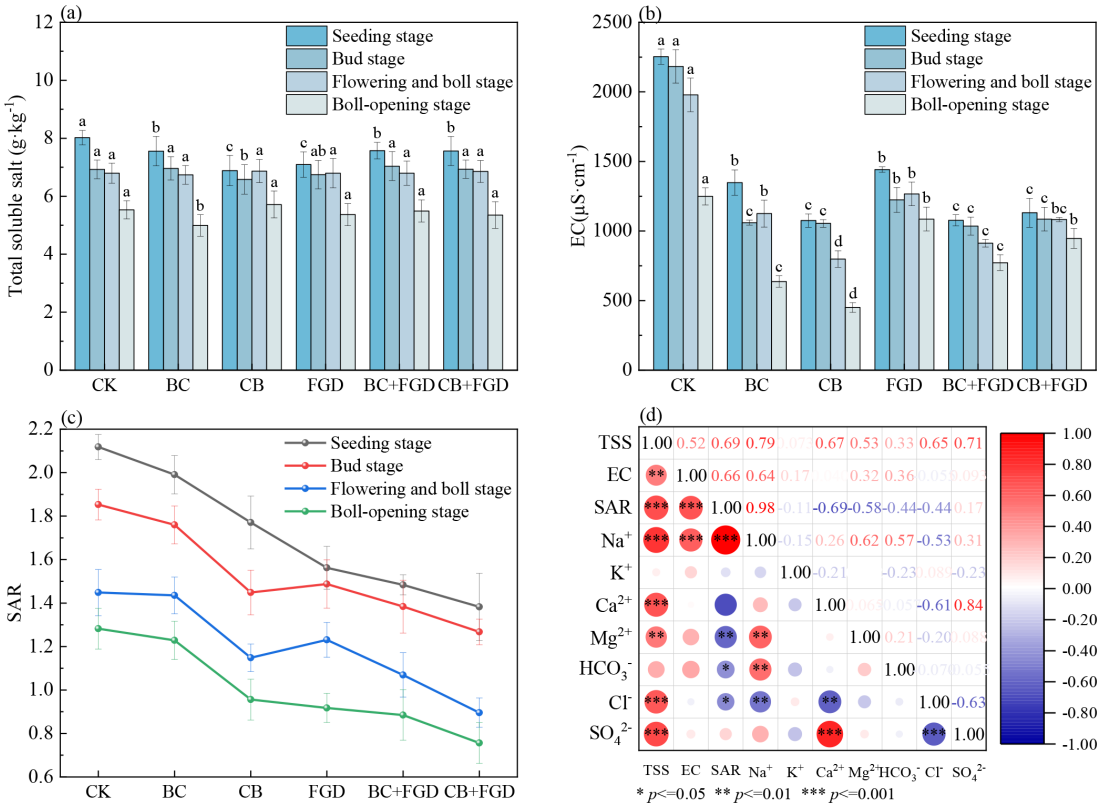

FIGURE 8
Total dissolved salts **(a)**, The electrical conductivity (EC) **(b)**, sodium adsorption ratio (SAR) **(c)** and their correlation analysis in saline soil at different growth stages of cotton **(d)**. The error bar represents ± standard deviation, and different lowercase letters indicate significant differences in different treatments at the same rinsing stage ($p < 0.05$).

carbon-based materials and FGD effectively reduced Na^+ content in the saline soil, with co-application proving superior. The CB+FGD treatment exhibited the strongest Na^+ suppression effect (Figure 4). This can be attributed to the porous structure and high SSA of carbon-based materials enabling effective adsorption of Na^+ (31). The CB, while retaining the inherent porous structure, significantly increases SSA (15), thereby enhancing Na^+ adsorption. Its improved water retention capacity also accelerates salt leaching (35). FGD provides supplemental Ca^{2+} to displace Na^+ from soil exchange sites (38).

FGD application significantly increased soil Ca^{2+} concentration. However, BC+FGD and CB+FGD co-applications showed no significant difference in Ca^{2+} and Mg^{2+} content compared to FGD alone, suggesting that Ca^{2+} and Mg^{2+} dynamics are primarily governed by FGD application (39, 40). Biochar and FGD supply polyvalent cations (e.g., Ca^{2+} and Mg^{2+}) and anions (e.g., SO_4^{2-}) (1, 2), which promote soil aggregate formation and soluble $MgSO_4$ generation (34). This enhances soil permeability and Mg^{2+} mobility, ultimately increasing leaching losses (21, 22). However, when co-applied with biochar, FGD's Mg^{2+}-mobilizing effect is significantly attenuated (30). Biochar achieves this by adsorbing/immobilizing Mg^{2+} ions and inducing precipitation through pH modification (23, 35). BC and BC+FGD treatments resulted in higher soil K^+ levels than others, likely due to the inherent K^+ content of the biochar feedstock. Nevertheless, the porous structure of biochar can promote K^+ leaching, explaining the significantly higher K^+ content observed in the 20–30 cm layer compared to 0–20 cm. While Na^+ concentration decreased and Ca^{2+} and K^+ concentrations increased overall, all three ions generally exhibited higher concentrations with increasing soil depth. This indicates that the amendments effectively modulated salt distribution within the profile. Irrigation during the crop growth period aids in leaching salts from the soil surface, representing a primary desalination phase in arid farmland (41). Our findings align with studies showing biochar enhances water retention and reduces salinity in the 0–40 cm layer (27), and that straw interlayers improve leaching efficiency by reducing infiltration rates (42).

The test soil was classified as chloride-sulfate saline soil (43). After leaching, Cl^- content was significantly reduced in the 0–20 cm layer, with CB+FGD showing the largest decrease. Conversely, FGD, BC+FGD, and CB+FGD treatments increased SO_4^{2-} content, potentially transforming the topsoil (0–20 cm) towards sulfate dominance. This demonstrates that both amendments promote Cl^- leaching (25, 44). The significant increase in Cl^- within the 20–30 cm layer (Figure 5) indicates downward migration of surface Cl^- with percolating water, increasing salinity in the subsoil (27). Extensive research confirms that carbon-based materials possess lower bulk density and more developed pore structures than saline soils. By enhancing soil water content and

infiltration capacity, they accelerate desalination (7, 35, 45). The chitosan-modified CB, containing more hydrophilic functional groups and exhibiting better hydrophilicity and polarity, increased soil water retention capacity by 23% compared to BC (15), contributing to its higher desalination efficiency.

While co-application increased SO_4^{2-} leaching, it also elevated SO_4^{2-} content in the post-leaching soil. This shift from potentially harmful carbonates and bicarbonates to less detrimental sulfates can be beneficial (39). FGD co-application significantly reduced HCO_3^- in the 0–20 cm layer but led to its accumulation in the 20–30 cm layer. This phenomenon may relate to the precipitation-dissolution equilibrium of $CaCO_3$, soil ion adsorption, exchange equilibria, and the decomposition of carbonate minerals to maintain electrostatic equilibrium (40). In summary, the application of carbon-based materials, particularly the chitosan-modified CB, significantly improved the physicochemical properties of the topsoil. By reducing harmful ions (Na^+, Cl^-) and increasing beneficial ions for plant growth (K^+, Ca^{2+}, SO_4^{2-}), it mitigated salt accumulation in the surface layer.

4.3 Dynamics of salt ions in field soil

Soil salinity is a major environmental factor influencing crop growth, directly impacting seedling emergence, plant development, and ultimately yield (7). Field trial results showed that Na^+ content decreased progressively during the cotton growth period but increased with soil depth. Ca^{2+} content also decreased over time, potentially linked to cotton root uptake for cell wall synthesis and osmotic regulation (46). Co-application outperformed single applications in maintaining Ca^{2+} availability; FGD provides a sustained Ca^{2+} release, while surface functional groups (e.g., carboxyl, hydroxyl) on the carbon-based materials reduce Ca^{2+} leaching to deeper layers via electrostatic adsorption, preserving its effectiveness in the topsoil (1). HCO_3^- content reached its minimum at the boll-opening stage, possibly due to reduced evaporation shifting the carbonate system equilibrium towards CO_2 release (47). Cl^- content in the 0–20 cm layer increased during the growth period and rose significantly with depth. Both amendments significantly increased SO_4^{2-} content, with CB+FGD showing the largest increase, consistent with the leaching experiment results. This pattern confirms that irrigation inputs during cotton growth drive the downward migration of surface salts with percolating water (41).

Co-application treatments consistently maintained lower Na^+ and Cl^- content across all soil layers and growth stages compared to single applications. Ca^{2+} supplied by FGD displaces Na^+ from soil colloids via ion exchange (38), reducing soil sodium saturation and enhancing permeability. This facilitates the leaching of ions with water towards deeper soil layers (41). The co-application effect of carbon-based materials and FGD was particularly pronounced in the topsoil (0–20 cm), potentially linked to biochemical processes in the root-dense zone, such as root exudates activating functional groups on the carbon materials (26). The CB, functioning as a soil amendment, contains a higher density of hydrophilic and cation-binding groups (e.g., carbonyl, hydroxyl, quaternary ammonium) (19) and exhibits exceptional water absorption and retention properties (15). These characteristics synergistically enhance salt ion leaching efficiency.

As the cotton grew and fertilization proceeded, soil K^+ content increased notably. The abundant hydroxyl groups on the polymer network of the superabsorbent CB can release H^+ (15), displacing and adsorbing K^+ from the soil solution. This sequesters K^+ within the material's surface and internal structure, reducing its loss and promoting retention. Concurrently, the improved soil moisture environment fostered by CB application enhanced cotton growth and root development. Increasing root exudates likely stimulated the release of slow-release or insoluble potassium into the soil solution, contributing to the rise in K^+ (19). Furthermore, most Na^+ and K^+ in the soil exist in free ionic forms (45), and an antagonistic relationship exists between them (48). Their absolute and relative quantities exhibited opposing trends over time, persisting until the end of the cotton growth period. The superabsorbent CB can reduce pore water salinity by binding salt ions within its polymeric chain structure, thereby mitigating salt ion accumulation and their detrimental effects on crops. Additionally, sole reliance on FGD for reclamation can lead to seasonal fluctuations in salinity. During high-temperature periods with low soil moisture, weak leaching, and strong evaporation, salt ions migrate upwards with evaporating water, causing surface salt accumulation. The superabsorbent CB counters this by enhancing soil water retention, improving water use efficiency, and suppressing evaporation. This effectively inhibits seasonal salt resurfacing and reduces harmful ion concentrations in the topsoil. Therefore, the co-application of superabsorbent carbon-based material and FGD is advantageous for reclaiming saline cotton fields and promoting sustainable agriculture in arid and semi-arid regions.

4.4 Dynamics of soil physicochemical properties

Salinity directly affects soil nutrient availability and crop growth (14). The highly significant positive correlation ($p < 0.01$) between TSS and EC confirms their mutual utility in characterizing soil salinity, with EC serving as a reliable rapid indicator (7). The significant reduction in TSS at the seedling stage by carbon-based materials and FGD is closely linked to the strong adsorption capacity and ion exchange functionality of the carbon materials (15). The single CB application showed the largest TSS decrease. In co-application treatments, the carbon material may buffer the rapid dissolution of FGD, delaying salt release and resulting in a relatively smaller TSS reduction (25). The TSS reduction from single FGD application was lower than from single carbon material application, likely because Ca^{2+} and Mg^{2+} released from dissolving FGD displace adsorbed Na^+ but simultaneously increase SO_4^{2-} content (38). The decrease in TSS and EC over the growth period is likely attributable to salt leaching induced by irrigation or precipitation (30). Other studies also report negative correlations between soil TSS/EC and biochar application (10, 25).

The significant reduction in SAR observed in the co-application treatment (CB+FGD) provides key evidence for the reduced effect

of sodicity risk by carbon-based materials and FGD. The strong positive correlations ($p < 0.001$) of Na^+, Ca^{2+}, Cl^-, and SO_4^{2-} with TSS identify them as the primary contributors to salinity. The strong positive correlation between SAR and Na^+, coupled with negative correlations with Ca^{2+} and Mg^{2+}, confirms the antagonistic role of Ca^{2+} and Mg^{2+} in counteracting Na^+ toxicity. The lack of significant correlation between K^+ and salinity indicators suggests that K^+ is primarily adsorbed or preferentially taken up by plants, contributing to osmotic adjustment rather than exacerbating soil salt stress (10). This study elucidates the mechanisms by which carbon-based materials and FGD achieve efficient amelioration of the 0–20 cm soil layer through regulating key ion balances and soil solution chemistry. Future research should investigate the long-term effects of these amendments on soil microbial communities, nutrient cycling, and plant physiology to refine the theoretical framework for saline soil ecological restoration.

5 Conclusion

This study investigated the ameliorative effects of co-applying a superabsorbent carbon-based material with FGD on saline-alkali soil. The results demonstrate that the application of carbon-based materials and FGD significantly enhanced salt ion leaching, effectively mitigating salt stress in saline soils of arid and semi-arid regions. The CB+FGD co-application treatment proved most effective, significantly reducing Na^+ and Cl^- content, increasing concentrations of K^+, Ca^{2+}, and SO_4^{2-}, and reducing salt accumulation in the topsoil.

1. Co-application of the superabsorbent carbon-based material and FGD significantly alleviated salt stress by promoting Na^+ leaching (co-application > single application). During the P1 (rapid decline) leaching phase, FGD alone and CB+FGD increased Na^+ leaching concentration by 89.08% and 90.92%, respectively. FGD co-application significantly increased soil Ca^{2+} and SO_4^{2-} content. The superabsorbent carbon-based material effectively retained soil K^+, and post-leaching Cl^- content was significantly lower than in the CK.
2. Field trials further confirmed that co-application of the superabsorbent carbon-based material and FGD significantly reduced Na^+, Cl^-, and Mg^{2+} content while increasing Ca^{2+}, K^+, and SO_4^{2-} content. The increasing concentrations of Na+, Cl^-, and K^+ with soil depth indicate the migration of salts towards deeper soil layers with water movement.
3. The CB+FGD treatment significantly reduced TSS, EC, and SAR, thereby improving key physicochemical properties of the saline soil.

These results provide a scientific basis for optimizing the application of CB and FGD in saline-alkali soil remediation. Future studies should integrate long-term monitoring of multi-dimensional soil indicators (physical, chemical, and biological), coupled with plant physiological responses, to comprehensively elucidate the mechanisms and sustainability of CB-FGD co-application under field conditions.

Data availability statement

The original contributions presented in the study are included in the article/Supplementary Material. Further inquiries can be directed to the corresponding author.

Author contributions

SZ: Writing – original draft, Methodology, Conceptualization. YY: Writing – original draft. JZ: Formal Analysis, Visualization, Writing – review & editing, Funding acquisition. XQ: Writing – review & editing, Data curation.

Funding

The author(s) declare that financial support was received for the research and/or publication of this article. This work was supported by the National Natural Science Foundation of China (42275014; 51569030), Bingtuan Guiding Science and Technology Plan Program (2024ZD098), President's foundation of Tarim University (TDZKCX202404, TDZKSS202156), and Bingtuan Science and Technology Program (2021DB019; 2022CB001-01; 20240231).

Acknowledgments

We gratefully acknowledge the support of the Instrumental Analysis Center in Tarim University.

Conflict of interest

The authors declare that the research was conducted in the absence of any commercial or financial relationships that could be construed as a potential conflict of interest.

Generative AI statement

The author(s) declare that no Generative AI was used in the creation of this manuscript.

Publisher's note

Supplementary material

The Supplementary Material for this article can be found online at: https://www.frontiersin.org/articles/10.3389/fsoil.2025.1639967/full#supplementary-material

References

1. Xu X, Wang J, Tang Y, Cui X, Hou D, Jia H, et al. Mitigating soil salinity stress with titanium gypsum and biochar composite materials: Improvement effects and mechanism. *Chemosphere*. (2023) 321:138127. doi: 10.1016/j.chemosphere.2023.138127

2. Negacz K, Malek Ž, De Vos A, Vellinga P. Saline soils worldwide: Identifying the most promising areas for saline agriculture. *J Arid. Environ*. (2022) 203:104775. doi: 10.1016/j.jaridenv.2022.104775

3. Zhang S, Wang L, Gao J, Zhou B, Hao W, Feng D, et al. Effect of biochar on biochemical properties of saline soil and growth of rice. *Heliyon*. (2024) 10:e23859. doi: 10.1016/j.heliyon.2023.e23859

4. Zhang S, Xue L, Liu J, Xia L, Jia P, Feng Y, et al. Biochar application reduced carbon footprint of maize production in the saline–alkali soils. *Agriculture Ecosyst Environment*. (2024) 368:109001. doi: 10.1016/j.agee.2024.109001

5. He H, Li D, Wu Z, Wu Z, Hu Z, Yang S. Assessment of the straw and biochar application on greenhouse gas emissions and yield in paddy fields under intermittent and controlled irrigation patterns. *Agriculture Ecosyst Environment*. (2024) 359:108745. doi: 10.1016/j.agee.2023.108745

6. Dai L, Fu R, Guo X, Du Y, Zhang F, Cao G. Soil moisture variations in response to precipitation across different vegetation types on the northeastern qinghai-tibet plateau. *Front Plant Sci*. (2022) 13:854152. doi: 10.3389/fpls.2022.854152

7. Yan S, Zhang S, Yan P, Wei Z, Wang H, Zhang H, et al. Biochar application strategies mediating the soil temperature, moisture and salinity during the crop seedling stage in Mollisols. *Sci Total Environ*. (2025) 958:178098. doi: 10.1016/j.scitotenv.2024.178098

8. Murtaza G, Usman M, Ahmed Z, Hyder S, Alwahibi MS, Rizwana H, et al. Improving wheat physio-biochemical attributes in ciprofloxacin-polluted saline soil using nZVI-modified biochar. *Ecotoxicology Environ Safety*. (2024) 286:117202. doi: 10.1016/j.ecoenv.2024.117202

9. Wu W, Zhen Z, Yang G, Yang C, Song M, Li X, et al. Straw biochar improves rice yield by regulating ammonia-oxidizing microorganisms and physicochemical properties of subtropical saline soils by a pot study. *Environ Technol Innovation*. (2025) 38:104204. doi: 10.1016/j.eti.2025.104204

10. Qiu Y, Wang Y, Zhang Y, Zhou L, Xie Z, Zhao X. Effects of adding different types and amounts of biochar to saline alkali soil on its salt ions and microbial community in northwest China. *iScience*. (2025) 28:112285. doi: 10.1016/j.isci.2025.112285

11. Ma Z, Yang Y, Wu Y, Xu J, Peng H, Liu X, et al. In-depth comparison of the physicochemical characteristics of bio-char derived from biomass pseudo components: Hemicellulose, cellulose, and lignin. *J Anal Appl Pyrolysis*. (2019) 140:195–204. doi: 10.1016/j.jaap.2019.03.015

12. Alghamdi AG, Alkhasha A, Ibrahim HM. Effect of biochar particle size on water retention and availability in a sandy loam soil. *J Saudi Chem Soc*. (2020) 24:1042–50. doi: 10.1016/j.jscs.2020.11.003

13. Verheijen FGA, Zhuravel A, Silva FC, Amaro A, Ben-Hur M, Keizer JJ. The influence of biochar particle size and concentration on bulk density and maximum water holding capacity of sandy vs sandy loam soil in a column experiment. *Geoderma*. (2019) 347:194–202. doi: 10.1016/j.geoderma.2019.03.044

14. Zhou Z, Li Z, Zhang Z, You L, Xu L, Huang H, et al. Treatment of the saline-alkali soil with acidic corn stalk biochar and its effect on the sorghum yield in western Songnen Plain. *Sci Total Environ*. (2021) 797:149190. doi: 10.1016/j.scitotenv.2021.149190

15. Yang Y, Zhong M, Bian X, You Y, Li F. Preparation of carbon-based material with high water absorption capacity and its effect on the water retention characteristics of sandy soil. *Biochar*. (2023) 5:61. doi: 10.1007/s42773-023-00260-8

16. Ai F, Yin X, Hu R, Ma H, Liu W. Research into the super-absorbent polymers on agricultural water. *Agric Water Manage*. (2021) 245:106513. doi: 10.1016/j.agwat.2020.106513

17. Piroonpan T, Haema K, Hiangrat K, Sriroth K, Pasanphan W. Sugarcane bagasse cellulose-PAA micro-composite super-water absorbent for sandy soil amendment: Exploring a complete set of studies from one-pot electron beam processing to pot-testing. *Ind Crops Prod*. (2024) 221:119219. doi: 10.1016/j.indcrop.2024.119219

18. Yang Y, Wu J, Zhao S, Gao C, Pan X, Tang DWS, et al. Effects of long-term super absorbent polymer and organic manure on soil structure and organic carbon distribution in different soil layers. *Soil Tillage Res*. (2021) 206:104781. doi: 10.1016/j.still.2020.104781

19. Zheng H, Mei P, Wang W, Yin Y, Li H, Zheng M, et al. Effects of super absorbent polymer on crop yield, water productivity and soil properties: A global meta-analysis. *Agric Water Manage*. (2023) 282:108290. doi: 10.1016/j.agwat.2023.108290

20. Sun Y, Wang X, Yao R, Xie W. Increasing sunflower productivity by mitigating soil salt stress through biochar-based amendments. *Arch Agron Soil Sci*. (2024) 70:1–16. doi: 10.1080/03650340.2024.2373163

21. Wang Y, Wang Z, Liang F, Jing X, Feng W. Application of flue gas desulfurization gypsum improves multiple functions of saline-sodic soils across China. *Chemosphere*. (2021) 277:130345. doi: 10.1016/j.chemosphere.2021.130345

22. Zhang Y, Yang J, Yao R, Wang X, Xie W. Short-term effects of biochar and gypsum on soil hydraulic properties and sodicity in a saline-alkali soil. *Pedosphere*. (2020) 30:694–702. doi: 10.1016/S1002-0160(18)60051-7

23. Wang J, Zhao A, Ma F, Liu J, Xiao G, Xu X. Amendment of saline–alkaline soil with flue-gas desulfurization gypsum in the yinchuan plain, northwest China. *Sustainability*. (2023) 15:8658. doi: 10.3390/su15118658

24. Ma S, Zhu Q, Zhang S, Zhen J. Biochar-composite methyl cellulose-coated slow-release materials for amelioration of soda saline soils. *J Environ Chem Eng*. (2025) 13:116003. doi: 10.1016/j.jece.2025.116003

25. Ebrahim Yahya K, Jia Z, Luo W, YuanChun H, Ame MA. Enhancing salt leaching efficiency of saline-sodic coastal soil by rice straw and gypsum amendments in Jiangsu coastal area. *Ain Shams Eng. J*. (2022) 13:101721. doi: 10.1016/j.asej.2022.101721

26. Wang X, Xia X, Riaz M, Babar S, El-Desouki Z, Qasim M, et al. Biochar amendment modulate microbial community assembly to mitigate saline-alkaline stress across soil depths. *J Environ Manage*. (2025) 385:125574. doi: 10.1016/j.jenvman.2025.125574

27. Xu Q, Xu Y, Xia H, Han H, Li M, Gong P, et al. Mitigation of soil salinity by biochar and halophytes. *Geoderma*. (2025) 454:117191. doi: 10.1016/j.geoderma.2025.117191

28. Hou Y, Chen Y, Ding J, Li Z, Li Y, Sun F. Ecological impacts of land use change in the arid tarim river basin of China. *Remote Sens*. (2022) 14:1894. doi: 10.3390/rs14081894

29. Li H, Wang W, Fu J, Wei J. Spatiotemporal heterogeneity and attributions of streamflow and baseflow changes across the headstreams of the Tarim River Basin, Northwest China. *Sci Total Environ*. (2023) 856:159230. doi: 10.1016/j.scitotenv.2022.159230

30. Yue Y, Guo W, Lin Q, Li G, Zhao X. Improving salt leaching in a simulated saline soil column by three biochars derived from rice straw (Oryza sativa L.), sunfower straw (Helianthus annuus), and cow manure. *J Soil Water Conserv*. (2016) 71:467–75. doi: 10.2489/jswc.71.6.467

31. He K, He G, Wang C, Zhang H, Xu Y, Wang S, et al. Biochar amendment ameliorates soil properties and promotes Miscanthus growth in a coastal saline-alkali soil. *Appl Soil Ecol*. (2020) 155:103674. doi: 10.1016/j.apsoil.2020.103674

32. Wan H, Qi H, Shang S. Estimating soil water and salt contents from field measurements with time domain reflectometry using machine learning algorithms. *Agric Water Manage*. (2023) 285:108364. doi: 10.1016/j.agwat.2023.108364

33. Tian Y, Xia R, Ying Y, Lu S. Desulfurization steel slag improves the saline-sodic soil quality by replacing sodium ions and affecting soil pore structure. *J Environ Manage*. (2023) 345:118874. doi: 10.1016/j.jenvman.2023.118874

34. Wallace M, Santos M, Silva MI, Airon J d A, Quintão A. Improved water and ions dynamics in a clayey soil amended with different types of agro-industrial waste biochar. *Soil Tillage Res*. (2022) 223:105482. doi: 10.1016/j.still.2022.105482

35. Xiao L, Meng F. Evaluating the effect of biochar on salt leaching and nutrient retention of Yellow River Delta soil. *Soil Use Manage*. (2020) 36:12638. doi: 10.1111/sum.12638

36. Ghassemi-Golezani K, Farhangi-Abriz S. Improving plant available water holding capacity of soil by solid and chemically modified biochars. *Rhizosphere*. (2022) 21:100469. doi: 10.1016/j.rhisph.2021.100469

37. Wang J, Yuan G, Lu J, Wu J, Wei J. Effects of biochar and peat on salt-affected soil extract solution and wheat seedling germination in the Yellow River Delta. *Arid Land Res Manage*. (2019) 34:1–19. doi: 10.1080/15324982.2019.1696423

38. Zhang W, Zhang W, Zhao Y, Wang S, Liu J, Li Y, et al. Practical application of high-sodicity wasteland reclamation with flue gas desulfurization gypsum in the Songnen Plain of China. *Land Degradation Dev*. (2022) 33:3652–7. doi: 10.1002/ldr.4412

39. Tian T, Zhang C, Zhu F, Yuan S, Guo Y, Xue S. Effect of phosphogypsum on saline-alkalinity and aggregate stability of bauxite residue. *Trans Nonferrous Metals Soc China*. (2021) 31:1484–95. doi: 10.1016/S1003-6326(21)65592-9

40. dos Santos WM, Gonzaga MIS, da Silva JA, de Almeida AQ, de Jesus Santos JC, Gonzaga TAS, et al. Effectiveness of different biochars in remediating a salt-affected Luvisol in Northeast Brazil. *Biochar*. (2021) 3:149–59. doi: 10.1007/s42773-020-00084-w

41. Liu N, Li Y, Cong P, Wang J, Guo W, Pang H, et al. Depth of straw incorporation significantly alters crop yield, soil organic carbon and total nitrogen in the North China Plain. *Soil Tillage Res*. (2021) 205:104772. doi: 10.1016/j.still.2020.104772

42. Li M, Wang W, Wang X, Yao C, Wang Y, Wang Z, et al. Effect of straw mulching and deep burial mode on water and salt transport regularity in saline soils. *Water*. (2023) 15:3227. doi: 10.3390/w15183227

43. Lyu N, Shl L, Dal Y, Li Y, Yin F. Reclamation of saline-alkali soils in Xinjiang: A reviewly. *J Irrigation Drainage*. (2024) 43:1–10. doi: 10.13522/j.cnki.ggps.2024074

44. Babar S, Baloch A, Qasim M, Wang J, Wang X, Iqbal R, et al. Unearthing the potential of aluminum-modified biochar for saline-alkali soil rejuvenation and microbial diversity enhancement. *Pedosphere*. (2025). doi: 10.1016/j.pedsph.2025.01.003

45. Cui L, Liu Y, Yan J, Hina K, Hussain Q, Qiu T, et al. Revitalizing coastal saline-alkali soil with biochar application for improved crop growth. *Ecol Eng*. (2022) 179:106594. doi: 10.1016/j.ecoleng.2022.106594

46. Saifullah, Dahlawi S, Naeem A, Rengel Z, Naidu R. Biochar application for the remediation of salt-affected soils: Challenges and opportunities. *Sci Total Environ*. (2018) 625:320–35. doi: 10.1016/j.scitotenv.2017.12.257

47. Duan Y, Shang X, Tian R, Li W, Song X, Zhang D, et al. Suppressing a mitochondrial calcium uniporter activates the calcium signaling pathway and promotes cell elongation in cotton. *Crop J*. (2024) 12:411–21. doi: 10.1016/j.cj.2024.01.014

48. Murguía JR, Bellés J M, Serrano R. A salt-sensitive 3'(2'),5'-bisphosphate nucleotidase involved in sulfate activation. *Science*. (1995) 267:232–4. doi: 10.1126/science.7809627